A metallographic approach to the study of MgH2-Mg phase transformation

M. Vittori Antisari, A. Montone, N. Abazovic,[1] A. Aurora, M. Drvendzija,[2] M.R. Mancini, D. Mirabile Gattia, F. Pierdominici

ENEA, Department of Physical Methods and Materials, Research Centre of Casaccia, Via Anguillarese 301, 00123, Rome, Italy;[1]Vinca Institute of Nuclear Sciences, Laboratory of Radiation Chemistry and Physics, Belgrade, 11000, Serbia; [2]permanent address: Vinca Institute of Nuclear Sciences, Laboratory of Material Sciences, Belgrade, 11000, Serbia

Corresponding author: Amelia Montone,

ENEA, Department of Physical Methods and Materials, Research Centre of Casaccia,

Via Anguillarese 301, 00123, Rome, Italy

Fax +39.06.30483176

E-mail: montone@casaccia.enea.it

Summary

An experimental protocol for the metallographic study of the phase transformation in the MgH2-Mg hydrogen storage system has been developed. To this purpose partially desorbed MgH2 powders have been examined by scanning electron microscopy, with the aim of better understanding the kinetic mechanisms involved in the thermal decomposition of MgH2 that is at the basis of H2 release. The method is based on the different secondary electron emission yield of metallic Mg and insulating MgH2 at low accelerating voltage. In optimized observation conditions, a net contrast between the two phases, even in the presence of catalyst particles constituted by heavy elements, has been obtained. First results evidence the role of catalyst particles in assisting the nucleation step in the MgH2/Mg phase transformation.

Keywords: Hydrogen storage; Magnesium hydride; Scanning Electron Microscopy; Microstructure; Metallographic analysis; Phase Transformation.

Introduction

Metallic hydrides are considered a priority material for the solid-state H2 storage owing to the high hydrogen capacity both by weight and by volume. Technological application in mobile storage of these potential "high H2 density" materials still shows several difficulties, often related to the H2 desorption temperature, to the low rates of H2 release-uptake and, in the case of the so called chemical hydrides, the soaking-releasing processes which are not reversible [1, 2].

Among the hydrides, the light-weighted MgH2 is one of the most promising and studied systems due to its reversibility in the desorption/absorption cycling, to the particularly high gravimetric H2 storage capacity, to its negative enthalpy of mixing, and to the low cost and high abundance. On the basis of literature results, it has been ascertained that the addition of a catalyst and the processing by high energy ball-milling appear necessary steps in order to reduce the decomposition temperature and to fasten the kinetics of the reaction. The effect appears to be related to the fine dispersion of catalyst particles inside the MgH2 matrix and to the introduction of high density of extended defects, which can assist the H2 diffusion throughout the material [3, 4].

Structural information on the phase transformation are usually obtained by X-ray and neutron diffraction while the calorimetric and thermo-gravimetric methods are commonly used to measure the efficiency of the powders in term of storage capacity and the rate of hydrogen sorption / release reactions. Isothermal decomposition experiments can be used to study the rate limiting step of the reaction, even if the interpretation of the results is often not completely unambiguous and can show a limited reliability [5,6]. All these methods describe the average behavior of the material. For example, features such as the nucleation sites and structure of the inter-phase boundaries are only indirectly derived, while this kind of information could be usefully obtained by

the microscopic observation of partially transformed samples. In the case of Mg/MgH$_2$ system, however, the metallographic approach is almost unexplored, even if the involved phases show optical and structural differences that can be the basis of a detectable and meaningful contrast in most experimental situations. In fact MgH$_2$ is an insulating transparent phase, while Mg is a conducting metal reflecting the visible light. These features can be at the bases of a detectable contrast both in optical microscopy and in Scanning Electron Microscopy. In the last case the contrast can be related to higher secondary electron yield generally shown by insulating phases with respect to the conducting ones [7].

Consequently, in suitable conditions SEM could be used to image the fine details of the microstructure in the binary Mg-MgH$_2$ system or in a ternary system where also a catalyst is present. Of course, the internal microstructure of the powder sample has to be exposed, so that an embedding and polishing procedure resulting in flat, polished, cross sectional samples has to be developed. However, the usual embedding procedure, based on the use of epoxy resin, does not appear suitable to the purpose. In fact the resulting sample is insulating and it has to be coated for SEM observation. The SE yield becomes so related to the structure of the coating film and the difference among the involved phases is lost. As it will be explained later, we have found a solution to this problem by embedding the powders in a metallic matrix and by observing the sample at low accelerating voltage.

In conclusion, the purpose of this paper is to describe an experimental protocol, including sample preparation and observation conditions, that allows to study the microstructure of partially decomposed, ball-milled MgH$_2$ samples by mean high resolution Scanning Electron Microscopy. Preliminary results on Fe catalyzed MgH$_2$ powder, here reported, support the usefulness of the approach in the study of the phase transformation, elucidating also the role of Fe catalyst particles.

Experimental

MgH$_2$ was provided by Th. Goldschmidt (95%, 60 mm particle size) and Fe by Noah Chemical (99,95%, 200 mesh). The MgH$_2$ powder was milled for 10h in a stainless steel vial in a Spex 8000 mixer-mill, under 2.5 bar of Argon atmosphere with a ball to powder ratio of 10:1. The catalyzed

sample was obtained by adding 10 wt% Fe powder to the MgH$_2$ powder. The powder manipulation was carried out in a MBraum MB10 Compact drybox system under inert Ar atmosphere (O$_2$<0,1 ppm, H$_2$O<0,2 ppm) in order to avoid contact of the sample with O$_2$ and humidity during the powders handling. The ball milled powders were partially desorbed by an interrupted temperature scan in a thermo-gravimetric apparatus under constant Ar flow. To this purpose the heating furnace was shut off when the desired amount of hydrogen was released. The resulting powders are constituted by a mixture of MgH$_2$ (un-reacted phase) and Mg (reacted phase), with the presence of Fe particles in the case of the catalyzed sample. With the purpose of a SEM observation, all the powders were embedded in an aluminum matrix, following a procedure already optimized for the TEM observation [8]. The partially desorbed powder was placed between two high purity Al foils (1 mm thick and with the size of 5x5 mm) and pressed at 20MPa by a hand driven press, until the cold welding was obtained. The resulting composite is cut to the original size and the whole procedure is repeated until the foil thickness is reduced to about 0.1 mm. In this way the powder particles are trapped in the Al matrix and their cross-section can be easily exposed by traditional metallographic preparation. The polishing steps was carried out by abrasives diamond pastes with decreasing size, while final surface preparation was by low-angle Ar ion beam milling in a Gatan PIPS system (3 kV beam energy, 5 degrees of incident angle and 30 minutes of milling).

The samples were observed by a Cambridge 250 MKIII SEM equipped with a solid state BSE detector.

Experimental method and results

Before entering in the experimental details, it is useful to briefly describe the strategy at the basis of our approach. As we shall see later, the nature of the embedding medium plays a relevant role on the final result, since it deeply affects the resulting contrast. We want to remind that the samples under study are constituted by a fine mixture of three phases, namely MgH$_2$ and Mg with the presence of Fe in the case of catalyzed specimens.

One possible contrast mechanism can be based on the BSE yield, η, related to the average atomic number. BSE yields computed according to the

Table 1. Average atomic number and BS electron yields of the three phases under investigation, calculated according to reference [9].

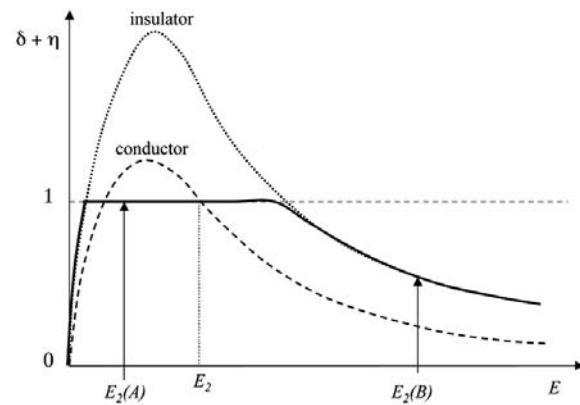| Phase	Average Z	BS Yield
MgH$_2$	4,7	0,096
Mg	12	0,19
Fe	26	0,33

Figure 1. Schematic representation of SE yield of a conducting (dash line) and insulating (dot line) phase vs. primary electron energy. The charge accumulation at the surface of the insulating phase influences the SE yield, so that, in steady state, the observed emission of an insulator follows the full line. The scheme is redrawn from curve reported in Cazaux J [7].

classical approach [9] are reported in Table 1.

As far as the SE yield is concerned, the typical behavior of the total electron yield of generic conducting and insulating phases at different accelerating voltages, has been recently reviewed by J. Cazaux [7]. Figure 1 reports the total electron emission yield of both insulating and metallic materials as a function of the accelerating voltage of the primary beam, as redrawn from the above cited paper. Neglecting the energy variation of the BSE contribution, this behavior can be representative of the SE emission. The SE yield shows a maximum larger than unity at low energy for both kind of materials and it decreases for higher primary energies, assuming values lower than unity. The insulating phase displays a SE yield larger than the metal in the whole energy range, owing to the larger escape depth of the secondary electron in this kind of material. Lets consider the behavior of an insulating phase around the critical primary energy, E$_2$, corresponding to the unity emission. Above this threshold, the insulating phase accumulates a negative charge at the surface which gives rise to image distortion and contrast artifacts in the SEM observation. On the contrary, below the threshold, a net positive charge accumulates at the surface. During a continuous irradiation, i.e. during a SEM observation, this charging reduces the SE emission yield until a steady state situation. In fact, the SE yield is progressively reduced by the positive surface charge until a unity total emission is reached, the charge balance at the surface becomes zero and consequently the surface neutrality is kept. This steady state behavior is described by the full line in Figure 2, which shows why uncoated insulators can be observed at low voltage without parasitic surface fields.

The comparison between the emission curves of the insulating and the conductive material evidences the presence of a contrast occurs both below

and above the critical energy, E$_2$. Below this threshold, the metal should appear brighter owing to a SE yield larger than unity with respect to the unity emission of the insulating phase, while at high voltage the contrast is reversed and the insulating phase should appear brighter than the metal. However, in this second case, image distortion and contrast anomalies can be expected, caused by the surface charging of the insulating phase, so that the observation at low accelerating voltage appears to represent the best experimental condition. However, the exploration of this kind of contrast requires a particular attention in the sample preparation. In fact, it is quite evident that any surface coating has to be avoided. Moreover, also the embedding in insulating media is not suitable to the purpose. In fact, in order to display the just described contrast, the sample has to allow an emission yield larger than unity from the metallic phase. This means that the net charge balance is different from zero and the excess charge has to be dispersed to ground in order to keep a steady state situation. This equilibrium can be maintained by embedding the powders in a conducting matrix where the ground contact is available to whichever part of the sample. In this way each phase can keep a behavior, as far as the SE yield is concerned, independent from each-other.

The above considerations have been tested on a sample containing a fine mixture of Mg, MgH$_2$ and Fe, obtained by partial thermal decomposition of

MgH_2 ball milled with Fe. The desorption process has been stopped when about 10% of MgH_2 was transformed to Mg, in order to study the first steps of the Mg nucleation process. Images in Figure 2 represent the typical contrast situation. In the BSE image (Figure 2a), the three gray levels correspond to the three phases with a brightness increasing with the average atomic number. The Mg based particles is clearly evident in the slightly heavier Al matrix. We only notice that the contrast between MgH_2 and Mg is very fable, probably because the reduced BSE detector amplification allowed by the signal saturation at the brighter Fe particles. This feature does not allow to image with high definition the distribution of these two phases. The contrast inversion at the critical voltage E_2 is evident by the comparison between the SE image taken at 20kV (Figure 2b) and the image taken below the threshold at 1kV (Figure 2c). It is also possible to observe that Figure 2b is affected by image distortion and contrast anomalies typical of surface charging, while the image at low voltage is free from any evident artifact and clearly displays the spatial distribution of the three phases. The smaller Fe particles are not evident in Figure 2c, probably owing to a reduced backscattering efficiency often observed at low primary energy electrons [10], so that the whole information about the sample microstructure can be obtained by integrating the information obtained by SE at low voltage, and by BSE at higher voltage. In this last case the information appears reliable owing to the relative insensitivity of this signal to the surface charging.

As far as the image contrast is concerned, it is quite surprising that the considerations about the independent emission of insulating and metallic phases hold also in the case of the present sample microstructure, where the metallic fraction appears completely embedded into the insulating one, so that the direct contact to the grounded matrix is not evident. We can suppose that a limited electrical conductivity of the insulator, coupled with the electrical capacity of the metallic phase are sufficient in keeping the surface neutrality of this last phase even in presence of a charge unbalance, as evidenced by the bright displayed contrast. On the other hand the absence of surface charging at the metals can be observed also in Figure 2b, evidencing that, in the situation of the SEM observation where each image point is subjected to periodic and impulsive irradiation, the metallic phases
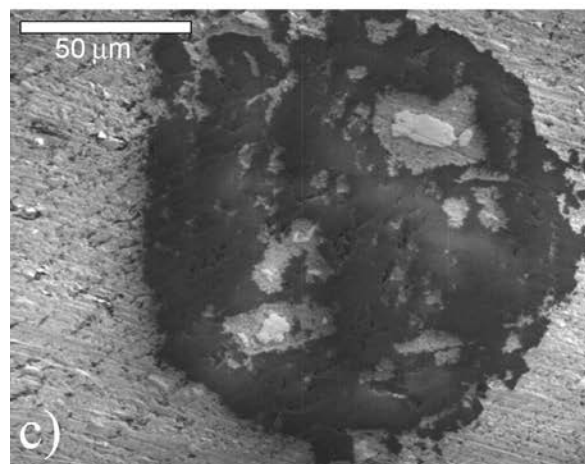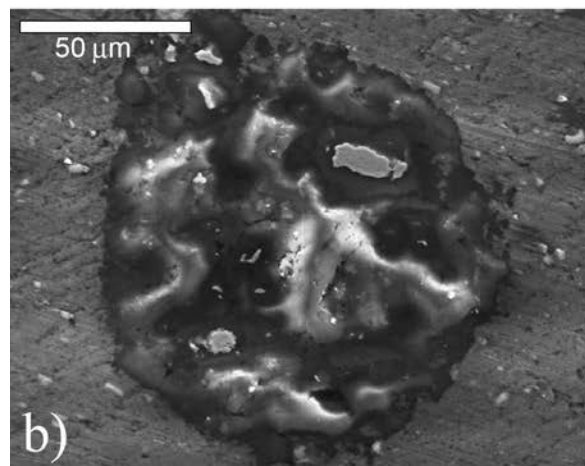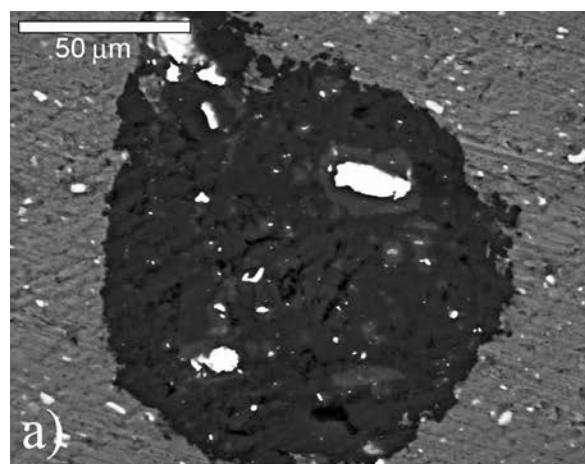

Figure 2. Series of images MgH_2 containing about 10wt% of Mg and Fe particles: a) BSE image at 20 kV; b) SE image at 20 kV and c) SE image at 1 kV.

can disperse the impinging current to ground also with the present microstructure.

Finally, coming back to the phase transformation from MgH_2 to Mg, we can notice how the Fe particles appear to be quite efficient in catalyzing the reaction. In fact, the metallic Mg is always located around Fe particles, evidencing the role of the last in assisting the nucleation step. It is worth noticing that nucleation inside the powder particles is quite unexpected in a situation where one of the resulting products is a gas which has to diffuse to the surface in order to reach its final state.

Conclusions

In this work a method to study the internal microstructure of $Mg-MgH_2$ samples at high spatial resolution is reported. The reactions of hydrating and dehydrating Mg can be successfully studied by this method and, in this work, preliminary observations on partially desorbed samples have been reported. The method is based on the different SE yield of the two phases, related to the difference in the electronic structure. The key point of the procedure is the embedding of the powder in a metallic matrix, which, besides allowing metallographic polishing to expose the particles cross sectional, supports the dispersion to the ground of the charge impinging on the conducting part of the sample. The experimental results can be interpreted on the basis of the expected contrast, even if a complete description of the effect, tacking into account the sample topography, has to be worked out. Owing to the reduced contrast between Mg and MgH_2 in BSE images and the small contrast displayed by Fe at low voltage, the complete information about the sample microstructure, with a detailed description of the phase distribution, can be obtained by integrating the information contained in the low voltage SE image with the high voltage BSE one.

References

1. Luo W. ($LiNH_2$–MgH_2): a viable hydrogen storage system, J Alloys Compd 2004;381:284-287.
2. Pinkerton FE, Meisner GP, Meyer M, Balogh M, Kundrat M. Hydrogen desorption exceeding ten weight percent from the new quaternary hydride $Li_3BN_2H_8$. J Phys Chem B 2005;109:6-8.
3. Huot J, Liang G, Boily S, Neste AV, Schulz R. Structural study and Hydrogen sorption kinetics of ball-milled magnesium hydride, J Alloys Compd 1999;293-295:495-500.
4. Oelerich W, Klassen T, Bormann R. Metal oxides as catalysts for improved hydrogen sorption in nanocristalline Mg-based materials, J. Alloys Compd 2001;315: 237-242.
5. Avrami M, Kinetics of phase change I, J Chem Phys 1939;7:1103-1112.
6. Avrami M, Kinetics of phase change II, J Chem Phys 1940;8:212-224.
7. Cazaux J. Charging in scanning electron microscopy "from inside and outside", Scanning 2004;26:181-203.
8. Montone A, Vittori Antisari M. A new method for preparing powders for transmission electron microscopy examination. Micron 2003;34:79–83.
9. Heinrich KFJ. X-ray optics and microanalysis, Castaing R, Dechamps P, and Philibert J, Paris, 1966
10. Frank L, Stekly R, Zadrazil M, El-Gomati MM, Mullerova I. Electron backscattering from real and in-situ treated surfaces, Mikrochimica Acta 2000;132:179-188.